IEEE Access
Multidisciplinary | Rapid Review | Open Access Journal

Received June 2, 2021, accepted June 13, 2021, date of publication June 17, 2021, date of current version June 24, 2021.

Digital Object Identifier 10.1109/ACCESS.2021.3090088

Robust Composite Adaptive Control of Linearisable Systems With Improved Performance

JENG-TZE HUANG, (Member, IEEE), AND YU-WEI JIANG
Institute of Digital Mechatronic Technology, Chinese Culture University, Taipei 11114, Taiwan

Corresponding author: Jeng-Tze Huang (hzz4@ulive.pccu.edu.tw)

This work was supported in part by the Ministry of Science and Technology, Taiwan, under Grant 109-2221-E-034 -003.

ABSTRACT Robust composite adaptive control designs for linearisable systems with known/unknown input gain functions are presented. They mainly consist of a standard adaptive linearizing controller and an immersion and invariance (I&I) based composite update algorithm, with the inclusion of a Lyapunov-based canceling term and a σ-modification term for ensuring the practical stability and preventing the parameter-drift phenomenon at the same time. Next, the adding an integrator and the dynamic surface control (DSC) techniques are incorporated for preventing the algebraic-loop problem in the latter case. In particular, the proposed designs ensure the convergence of prediction errors to an order of the exogenous disturbance without relying on persistent excitation (PE), which in turn improves the tracking performance significantly.

INDEX TERMS Adding an integrator, composite adaptive control, dynamic surface control, immersion and invariance, smooth switching.

I. INTRODUCTION

Adaptive control incorporating a Lyapunov-based update algorithm (LBUA) is now a standard tool for ensuring the asymptotic tracking stability of a dynamical system with parametric uncertainty [1], [2]. In the presence of bounded disturbances, various modification terms, such as the σ-modification, dead-zone, etc, can be included to ensure the practical tracking stability and to prevent the occurrence of the parameter-drift phenomenon simultaneously [2]. However, the online identification results are generally unsatisfactory due to the lack of prediction error terms in the LBUA. Intuitively, more accurate identification implies better tracking performance in practice.

Via either the filtering technique or a moving time window of online integration of the regressor vector for obtaining the prediction-error terms, versatile composite adaptive control (CAC) schemes are now available in the literature [1]–[9]. However, the former introduces extra dynamics which may deteriorate the transient performance, while the latter requires excessive computational burden. Alternatively, the I&I method is a non-uncertainty equivalent approach which results in a filter-free, gradient-type parameter estimator [10]–[12]. By incorporating the so-called dynamic regressor extension and mixing method [13], robust stability of the parameter error dynamics with finite-time convergence was achieved in [14], [15]. Noticeably, performance improvement in the aforementioned works relies on the parameter convergence, which in turn imposes various excitation criteria on the regressor vectors, such as PE [3]–[7], internal excitation (IE) [9], relaxed PE [13], [14], etc. Unfortunately, they are generally hard to verify beforehand [2], [11]. Accordingly, alternative approaches for performance improvement relaxing such criteria are in demand. In particular, issues regarding the convergence of the prediction errors (not parametric errors) in the presence of bounded disturbances and their influences on the tracking performance remain open so far.

In this regard, CAC designs for linearisable systems with known/unknown input-gain functions are presented in this article. The update algorithm is constructed via the I&I method with the inclusion of the LBUA and the σ-modification terms for ensuring the practical stability and the prevention of parameter-drift phenomenon at the same time. Meanwhile, the adding an integrator technique [16] and the DSC scheme are adopted for avoiding the possible

The associate editor coordinating the review of this manuscript and approving it for publication was Valentina E. Balas.

This work is licensed under a Creative Commons Attribution 4.0 License. For more information, see https://creativecommons.org/licenses/by/4.0/

algebraic-loop problems in cases when the input-gain functions are unknown. More significantly, by exploring the features of an invariant set with time-varying boundaries, it is shown that the prediction errors can be managed to an order of the exogenous disturbance without resorting to the aforementioned excitation criteria, which in turn improves the tracking performance in a systematic way. The contributions of the paper are summarized as follows

- Adaptive I&I control of a general linearisable system with known/unknown input gain functions under exogenous disturbances, to the best of our knowledge, is presented in the literature for the first time.
- Convergence of prediction errors and the corresponding performance improvement are quantitatively characterized. In particular, it is shown that such an achievement does not rely on PE or its variants, which facilitates its practical applicability.

The rest of the paper is organized as follows. The problem formulation is introduced in Section II. The proposed control and parametric estimator designs for cases with known/unknown input gain functions are detailed in Section III/IV, respectively. Simulation works for demonstrating the validity of the proposed designs follow up in Section V. Conclusion is drawn in Section VI.

II. PROBLEM FORMULATION

Consider the following n'th-order linearisable system

$$\begin{aligned} \dot{x}_1 &= x_2, \\ &\vdots \\ \dot{x}_{n-1} &= x_n, \\ \dot{x}_n &= g(x)u + \theta_f^T \phi_f(x) + d(t), \end{aligned} \tag{1}$$

where $x = [x_1, x_2, \cdots, x_{n-1}, x_n]^T \in R^n$ is the state vector; $u \in R$ is the control input; $g(x) : R^n \to R$ is the input-gain function; $\theta_f \in R^r$ is the unknown constant parameter vector; $\phi_f(x) : R^n \to R^r$ is the known regressor; and $d(t)$ is the exogenous disturbance input satisfying $|d(t)| \leq \epsilon$, with ϵ being an unknown positive constant.

This article aims to track a reference trajectory $x_d(t) = [x_d, \dot{x}_d, \cdots, x_d^{(n-1)}]^T$ for $x(t)$ via the adaptive I&I approach. The following assumptions are first made herein.

- *Assumption 1:* The whole state x is measurable.
- *Assumption 2:* The reference trajectory $x_d(t)$ is bounded and sufficiently smooth such that the signals $x_d^{(i)}, i = 0, \cdots, n$ are available.
- *Assumption 3:* The regressor $\phi_f(x)$ is differentiable with respect to its arguments.
- *Assumption 4:* $g(x)$ is a C^1 function bounded away from zero for all $x \in R^n$.

As mentioned, despite that various CAC schemes are now available in the literature, performance improvement of these works generally relies on the convergence of parameter errors, which in turn imposes certain excitation criteria on the regressor vectors that are hard to verify beforehand. To relax such restrictions, two I&I-based CAC designs are synthesized in the sequel.

III. CASES WITH KNOWN $g(x)$

We first consider the case where $g(x)$ is known exactly in this section. It starts with a standard adaptive linearizing control. An I&I-based update algorithm, modified from [11] and [12], is developed next. Stability analysis for the overall closed-loop system then follows up.

A. CONTROL LAW

To begin with, define the following auxiliary error variable [1]

$$S = (s + \lambda_0)^{n-1} e_1, \tag{2}$$

where $s = d/dt$, $\lambda_0 > 0$ is a constant, and $e = x - x_d = [e_1, \cdots, e_n]^T$.

Differentiating S in (2) with time, it results in

$$\dot{S} = g(x)u + \theta_f^T \phi_f(x) + d(t) + p(t), \tag{3}$$

where $p(t) = -x_d^{(n)} + \sum_{i=1}^{n-1} \binom{n-1}{i} \lambda_0^i s^{n-i} e_1$, with $\binom{n-1}{i}$ standing for the binomial coefficient.

By virtue of the exponential stability of the e_1 dynamics on the sub-manifold $S = 0$, control of the original n-dimensional system (1) has been reduced to the stabilization problem of the one dimensional S-dynamics in (3). To that end, the following adaptive linearizing control is adopted

$$u = \frac{1}{g(x)}(-k_s S - p(t) - \hat{\theta}_f^T \phi_f(x)) \tag{4}$$

where $k_s > 0$ is a gain constant and $\hat{\theta}_f$ is the estimated parameter vector for θ_f.

The resulting closed-loop system becomes

$$\dot{S} = -k_s S + \tilde{\theta}_f^T \phi_f(x) + d(t) \tag{5}$$

where $\tilde{\theta}_f = \theta_f - \hat{\theta}_f$.

For updating $\hat{\theta}_f$, the following LBUA is widely utilized

$$\dot{\hat{\theta}}_f = \gamma_0 S \phi_f(x) - \sigma \hat{\theta}_f \tag{6}$$

where $\gamma_0 > 0$ is the update gain and $-\sigma\hat{\theta}_f$ is the so-called σ-modification for preventing the parameter-drift phenomenon.

Next, by calculating the time derivative of the following Lyapunov function

$$V_1(S, \tilde{\theta}_f) = \frac{1}{2}(S^2 + \frac{1}{\gamma_0}\tilde{\theta}_f^T \tilde{\theta}_f) \tag{7}$$

along the closed-loop system (5) and (6), after some straightforward manipulations, it yields

$$\dot{V}_1 \leq -k_e V_1 + \frac{1}{2}(\epsilon^2 + \frac{\sigma}{\gamma_0}||\theta_f||^2) \tag{8}$$

where $k_e = \min(2k_s - 1, \sigma)$.

It can be easily seen from (8) that $S(t), \tilde{\theta}_f(t) \in L_\infty$, and for any $0 < c_0 < 1$, there exists a $T_0 > 0$, such that $|S| \leq ((1 + c_0)\delta_0/k_e)^{1/2}, \forall t \geq T_0$, where $\delta_0 = \epsilon^2 + (\sigma/\gamma_0)||\theta_f||^2$.

The ultimate boundedness of $e_i(t), i = 1, \cdots, n$ follows immediately [1]

$$|e_i(t)| \leq \frac{2^{i-1}}{\lambda_0^{n-i}} \sqrt{\frac{(1+c_0)\delta_0}{k_e}}, \quad \forall t \geq T_0 \tag{9}$$

Strictly speaking, an exponentially decaying transient term should be added to the right-hand side of (9) when $e(0) \neq 0$ [1]. However, since it decays rapidly to zero and is therefore neglected herein for simplicity and without loss of generality.

Despite its popularity, such an approach suffers from the following two drawbacks.

D1): The bound for $|\tilde{\theta}_f^T \phi_f(x)|$ and its influences on the tracking performance are not quantitatively characterized.

D2): To decrease the error bound in (9), the criteria of $k_e = \min(2k_s - 1, \sigma) \gg 1$ and $\gamma_0 \gg \sigma$ have to be fulfilled simultaneously, which may lead to poor transients or even high-adaptation instability when $\gamma_0 \gg \sigma \gg 1$ [2], [17].

In this regard, an I&I-based composite update algorithm (CUA) lifting these two restrictions is developed in the sequel.

Remark 1: Clearly, the more demanded asymptotic tracking stability can be attained via including a discontinuous control term, such as sign(S), for counteracting the disturbance $d(t)$ in (1). However, the unwanted chattering behavior may be ignited at the same time. To prevent its occurrence, a continuous approximation of sign(S), such as tanh(S), is generally adopted. However, only practical stability can be achieved instead [1], [21]. Besides, approximation errors are inevitable and therefore issues of performance improvement for a general robust adaptive control arise again. Consequently, the proposed design covers a wide variety of applications.

B. COMPOSITE UPDATE ALGORITHM

The adaptive I&I is a non-certainty equivalent approach which expresses the $\hat{\theta}_f$ in (4) as the sum of a deliberately selected design function $h_f(x) \in R^r$ and the estimated parameter vector $\vartheta_f(t) \in R^r$, i.e. [10], [11]

$$\hat{\theta}_f(t) \triangleq h_f(x) + \vartheta_f(t), \tag{10}$$

where

$$h_f(x) = \gamma \int_0^{x_n} \phi_f(x_1, \cdots, x_{n-1}, \xi) d\xi, \tag{11}$$

with $\gamma > 0$ being the gain constant, while $\vartheta_f(t)$ is updated by

$$\dot{\vartheta}_f(t) = -\sum_{k=1}^{n-1} \frac{\partial h_f(x)}{\partial x_k} x_{k+1} - \gamma_0 \{\gamma_1 [g(x)u + \hat{\theta}_f^T \phi_f]\phi_f - S\phi_f\} - \sigma \hat{\theta}_f \tag{12}$$

where $\gamma_1 = \gamma/\gamma_0$.

By a direct differentiation of (10) and taking (11)-(12) into account, it yields

$$\begin{aligned} \dot{\hat{\theta}}_f(t) &= \dot{h}_f(x) + \dot{\vartheta}_f(t) \\ &= \sum_{k=1}^{n} \frac{\partial h_f(x)}{\partial x_k} \dot{x}_k + \dot{\vartheta}_f(t) \\ &= \gamma_0 \{S\phi_f + \gamma_1 (\tilde{\theta}_f^T \phi_f + d(t))\phi_f\} - \sigma \hat{\theta}_f \end{aligned} \tag{13}$$

As can be seen, the first term of (12) cancels out the time derivative $dh_f(x)/dt$ to yield the desired remaining term $(\partial h_f(x)/\partial x_n)\dot{x}_n$. On the other hand, it is reminded that (13) is non-implementable and for the stability analysis only.

C. STABILITY ANALYSIS

Define

$$\begin{aligned} \rho_1 &= \sqrt{(1+c_1)[(1+\frac{1}{\gamma_1})\epsilon^2 + \frac{\sigma}{\gamma}||\theta_f||^2]} \\ \rho_2 &= \sqrt{\frac{(1+c_2)(\rho_1^2 + \epsilon^2)}{2(k_s - 1)}} \end{aligned} \tag{14}$$

where $0 < c_1, c_2 < 1$ are tunable constants.

The main results are summarized in the following.

Theorem 1: Consider the system (1), the controller (4), and the parametric estimator (10)-(12). For any bounded initial $(x(0), \hat{\theta}_f(0))$, the following properties are ensured if $k_s > 1$.

P1: $x(t), \hat{\theta}_f(t), u(t) \in L_\infty, \forall t \geq 0$;

P2: There exist a finite positive number T_1 and a $T_2 \geq T_1$, such that

$$|\tilde{\theta}_f^T \phi_f(x)| \leq \rho_1, \quad \forall t \geq T_1, \tag{15}$$

and

$$|e_i(t)| \leq \frac{2^{i-1}}{\lambda_0^{n-i}} \rho_2, \quad \forall t \geq T_2, \tag{16}$$

where $i = 1, \cdots, n$.

Proof:

The time derivative of $V(S, \tilde{\theta}_f)$ in (7), along the trajectories of the closed-loop system (5) and (13), can be calculated as follows

$$\begin{aligned} \dot{V}_1 &= S\dot{S} - \frac{1}{\gamma_0} \tilde{\theta}_f^T \dot{\hat{\theta}}_f \\ &= S(-k_s S + \tilde{\theta}_f^T \phi_f + d(t)) - S(\tilde{\theta}_f^T \phi_f) \\ &\quad -\gamma_1 (\tilde{\theta}_f^T \phi_f)(\tilde{\theta}_f^T \phi_f + d(t)) + \frac{\sigma}{\gamma_0} \tilde{\theta}_f^T \hat{\theta}_f \end{aligned} \tag{17}$$

By completing the squares, $Sd \leq 0.5(S^2 + \epsilon^2)$, $(\tilde{\theta}_f^T \phi_f)d \leq 0.5((\tilde{\theta}_f^T \phi_f)^2 + \epsilon^2)$, $\tilde{\theta}_f^T \hat{\theta}_f \leq 0.5(-\tilde{\theta}_f^T \tilde{\theta}_f + ||\theta_f||^2)$, and then substituting them into (17), it yields

$$\dot{V}_1 \leq -k_e V_1 - \frac{\gamma_1}{2} (\tilde{\theta}_f^T \phi_f)^2 + \frac{\delta_1}{2} \tag{18}$$

where $\delta_1 = (1 + \gamma_1)\epsilon^2 + (\sigma/\gamma_0)||\theta_f||^2$.

Define

$$b(t) = \max[0, \frac{(1+c_1)\delta_1 - \gamma_1(\tilde{\theta}_f^T\phi_f)^2}{2k_e}] \tag{19}$$

Consider the case when $b(t) = 0$, or equivalently, $\gamma_1(\tilde{\theta}_f^T\phi_f)^2 \geq (1+c_1)\delta_1$. Then (18) becomes

$$\begin{aligned}\dot{V}_1 &\leq -k_e V_1 - \frac{c_1\delta_1}{2} \\ &\leq -k_e(V_1 - b(t)) - \frac{c_1\delta_1}{2}\end{aligned} \tag{20}$$

Next consider the case when $b(t) > 0$, i.e. $\gamma_1(\tilde{\theta}_f^T\phi_f)^2 < (1+c_1)\delta_1$. By adding and subtracting $k_e b(t)$ to the righthand side of (18), it becomes

$$\dot{V}_1 \leq -k_e(V_1 - b(t)) - \frac{c_1\delta_1}{2} \tag{21}$$

Clearly, (20) and (21) together imply that $\dot{V}_1(t) \leq -c_1\delta_1/2$, $\forall V_1(t) \geq b(t), t \geq 0$. Since $V_1(t)$ decays with a speed no less than $c_1\delta_1/2$ when $V_1(t) > b(t)$, there then exists a positive number T_1 (depending on the initials) such that $(S, \tilde{\theta}_f) \in \Omega_1(t) = \{(S, \tilde{\theta}_f) | V_1(t) \leq b(t)\}, \forall t \geq T_1$. Conceptually, Ω_1 can be regarded as an invariant set with time-varying boundaries. Since $0 \leq b(t) \leq (1+c_1)\delta_1/2k_e$, it follows that $S(t), \hat{\theta}_f(t) \in L_\infty$ and consequently $x(t), u(t) \in L_\infty$. P1 is thus proven.

To prove (15), we only need to consider the case when $b(t) > 0, t \geq T_1$ since $b(t) = 0, t \geq T_1$ implies that $V_1(t) \leq 0$ and therefore $\tilde{\theta}_f^T\phi_f(x) = 0$. Under such circumstances,

$$\begin{aligned}(\tilde{\theta}_f^T\phi_f)^2 &\leq ||\tilde{\theta}_f||^2||\phi_f||^2 \\ &\leq 2\gamma_0||\phi_f||^2 V_1 \\ &\leq \frac{\gamma_0||\phi_f||^2[(1+c_1)\delta_1 - \gamma_1(\tilde{\theta}_f^T\phi_f)^2]}{k_e}\end{aligned} \tag{22}$$

and hence

$$\begin{aligned}\gamma_0(1+c_1)\delta_1||\phi_f||^2 &\geq (k_e + \gamma_0\gamma_1||\phi_f||^2)(\tilde{\theta}^T\phi_f)^2 \\ &\geq \gamma_0\gamma_1||\phi_f||^2(\tilde{\theta}^T\phi_f)^2\end{aligned} \tag{23}$$

The ultimate bound in (15) then follows immediately.

To see how the proposed estimation design affects the tracking performance, consider the Lyapunov function $V_2(S) = 0.5S^2$. Its time derivative along (5) can be calculated as

$$\begin{aligned}\dot{V}_2(S) &= S\dot{S} \\ &= S\{-k_s S + \tilde{\theta}_f^T\phi_f + d(t)\} \\ &\leq -(k_s - 1)S^2 + \frac{(\tilde{\theta}_f^T\phi_f)^2}{2} + \frac{d(t)^2}{2} \\ &\leq -2(k_s - 1)V_2 + \frac{\rho_1^2 + \epsilon^2}{2}, \quad \forall t \geq T_1.\end{aligned} \tag{24}$$

Therefore, given a positive number $0 < c_2 < 1$, there exists a $T_2 \geq T_1$, such that

$$|S(t)| \leq \rho_2, \quad \forall t \geq T_2. \tag{25}$$

Similar to (9), the results in (16) can be attained immediately.

Remark 2: The proposed design possesses the following advantages.

(i) The ultimate bound in (15) can be decreased to an order $\mathcal{O}(\epsilon)$ sustained that $(\sigma/\gamma)|\theta_f|^2 \ll 1$. Note that such a criterion does not necessarily imply a large γ, just a sufficiently small σ/γ ratio, e.g., $\sigma = 0.01$ and $\gamma = 1.0$. Under such circumstances, (15) can be approximated as

$$|\tilde{\theta}_f^T\phi_f| \leq \rho_1 \approx \sqrt{(1+c_1)(1+\gamma_1^{-1})}\epsilon \tag{26}$$

Accordingly, the drawback stated in D1 is conquered.

(ii) The ultimate tracking error bound in (16) can be arbitrarily decreased via using sufficiently large control gain k_s alone, which is apparently less restrictive than the criteria stated in D2.

(iii) The design in [11] was a disturbance-free modular design, which required the prior boundedness of $x(t)$. Via including the LBUA and the σ-modification terms herein, not only the aforementioned prerequisite is relaxed, but also the parameter-drift phenomenon is prevented at the same time.

(iv) The prediction errors in most of the existing CAC schemes are obtained via either the filtering technique [1], [3], [5]–[8] or a moving time window of online integration of the regressor vector, i.e. $Q(t) = \int_{t-\tau_d}^{t} \Phi(x(\tau))\Phi^T(x(\tau))d\tau$, where $\tau_d > 0$ is the width of the time window and $\Phi(x(t))$ is the regressor vector [4], [9]. As mentioned previously, the former introduces extra filter dynamics while the latter requires excessive computational burden. In contrast, the proposed CUA in (10)-(12) is a filter-free approach and hence conquers the drawback of the former. On the other hand, it is reminded that the term $Q(t)$ above can only be attained via a real-time integration. In contrast, the integration in (11) can be carried out off-line when $\phi_f(x)$ is integrable with respect to x_n. The computational burden of the former is alleviated under such circumstances. Most of all, the ultimate boundedness of $\tilde{\theta}_f^T\phi_f$ and its influence on the tracking performance can be quantitatively characterized with relative ease in the design herein.

IV. CASES WITH UNKNOWN $g(x)$

In this section, we consider the case where $g(x)$ is with linear parametric uncertainty in a form of $g(x) = \theta_g^T\phi_g(x)$, $\theta_g, \phi_g(x) \in R^m$ and $\phi_g(x)$ is differentiable in x. Moreover, we assume that

- *Assumption 5*: $g(x)$ fulfills

$$g_m \leq g(x) \leq g_u(x) \tag{27}$$

where $g_m > 0$ and $g_u(x) : R^n \to R_+ \in C^1$ are known *a priori*. Note that (27) covers the typical assumption in [19] where $g_u(x)$ is a positive number or the one in [6] with $g(x)$ being an unknown positive number.

A. EXISTING CAC ALGORITHM

With θ_g being unknown, the adaptive linearizing control in (28) becomes

$$u = \frac{1}{\hat{g}(t)}(-k_s S + \varphi(\hat{\theta}_f, x)), \tag{28}$$

where $\varphi(\hat{\theta}_f, x) = -\hat{\theta}_f^T \phi_f(x) - p(t)$, $\hat{g}(t) = \hat{\theta}_g^T(t)\phi_g(x)$, and $\hat{\theta}_g(t)$ is the estimation of θ_g.

Note that the so-called control singularity may occur when the denominator in (28) approaches zero. The smooth switching methodology in [18] can be invoked to bypass such a risk. The control law is now in a form of

$$u = -\frac{k_s}{g_m} S + B(\hat{g})u_a + (1 - B(\hat{g}))u_r, \tag{29}$$

where

$$u_a = \frac{1}{\hat{g}(t)}\varphi(\hat{\theta}_f, x),$$
$$u_r = -\frac{\varphi(\hat{\theta}_f, x)}{g_m}\tanh(\frac{S\varphi(\hat{\theta}_f, x)}{w_0}), \tag{30}$$

and $B(\cdot)$ is a switching function given by [18]

$$B(\zeta) \triangleq 1 - \exp(-(\zeta/w_s)^2), \tag{31}$$

with $w_0, w_s > 0$ and $\zeta \in R$.

By decreasing $B(\hat{g})$ continuously to zero, the control authority switches smoothly from the adaptive linearizing control u_a to the robust control u_r and vice versa. Note that the popular logic-based switching mechanism cannot be adopted herein for its non-differentiability at the switching point. Besides smoothness, $B(\zeta)$ possesses the following desired feature for annihilating the control singularity problem,

$$\frac{B(\zeta)}{\zeta} \le c_s/w_s, \quad \forall \zeta \in R \tag{32}$$

where $c_s \approx 0.64$.

By substituting (28)-(30) into (3), it yields the following closed-loop system

$$\dot{S} = -\frac{g}{g_m}k_s S + \tilde{\theta}^T\psi_s + d(t)$$
$$-(1 - B(\hat{g}))\varphi(1 + \frac{g}{g_m}\tanh(\frac{S\varphi}{w_0})) \tag{33}$$

where $\theta = col[\theta_f, \theta_g]$ and $\psi_s = col[\phi_f, (B(\hat{g})\varphi/\hat{g})\phi_g]$.

For updating $\hat{\theta}(t)$, the following CUA is widely adopted [6], [7]

$$\dot{\hat{\theta}}(t) = \gamma_0(S\psi_s + \gamma_1\tilde{x}_n) - \sigma\hat{\theta} \tag{34}$$

where $\tilde{x}_n = x_n - \hat{x}_n$ is the prediction error, with $\hat{x}_n$ being the output of the following serial-parallel identification model (SPIM) [2], [8]

$$\dot{\hat{x}}_n = -w_p\hat{x}_n + w_p x_n + \hat{\theta}_g^T\phi_g(x)u + \hat{\theta}_f^T\phi_f(x) \tag{35}$$

where $w_p > 0$ is a gain constant.

By subtracting the x_n dynamics in (1) from (35), $\tilde{x}_n$ can actually be expressed as

$$\tilde{x}_n = \frac{1}{s + w_p}[\tilde{\theta}_g^T\phi_g(x)u + \tilde{\theta}_f^T\phi_f(x) + d(t)] \tag{36}$$

As mentioned in (iv) of Remark 2, the extra filter dynamics in (35) may cause extra computation and discount the performance improvement. We are thus motivated to synthesize the I&I-based CAC design in the following.

B. CONTROL DESIGN

Before the start, the algebraic-loop problem, arising from the dependence of the design function $h(x, u)$ on $u(S, \hat{\theta})$, has to be resolved first. Among others, the adding an integrator technique in [16] is invoked herein. By inserting an integrator between the control input u and the system, the resulting extended system becomes

$$\begin{aligned}\dot{x}_1 &= x_2,\\ &\vdots\\ \dot{x}_n &= (\theta_g^T\phi_g)x_{n+1} + \theta_f^T\phi_f + d(t),\\ \dot{x}_{n+1} &= u\end{aligned} \tag{37}$$

with the corresponding S dynamics

$$\dot{S} = (\theta_g^T\phi_g)x_{n+1} + \theta_f^T\phi_f + p(t) + d(t), \tag{38}$$

It is noted that the uncertainty in (37) now becomes the extended-matching type as a price. The backstepping tool emerges as the best candidate for the control design [19], [20]. Define the state variable

$$z = x_{n+1} - q \tag{39}$$

where $q(t)$ is the output of the following first-order filter

$$\tau_0\dot{q}(t) + q(t) = \alpha(t), \quad q(0) = \alpha(0), \tag{40}$$

with $\tau_0 > 0$ and $\alpha(t)$ being the virtual controller at disposal.

The DSC technique above is mainly for preventing the algebraic-loop problem arising from the differentiation of α during the backstepping design procedure, which will be further clarified later on.

By replacing x_{n+1} in (38) with $(\alpha + z)$, followed by a direct differentiation of (39), the extended tracking error system can be rewritten as

$$\begin{aligned}\dot{S} &= (\theta_g^T\phi_g)(\alpha + z) + \theta_f^T\phi_f + d(t) + p(t) + g(x)\nu(t)\\ \dot{z} &= u - \dot{q}\end{aligned} \tag{41}$$

where $\nu(t) = q(t) - \alpha(t)$.

For stabilizing (41), the virtual/actual controllers are specified as follows

$$\alpha = -\frac{1}{g_m}[k_s + a_1 g_u(x)^2 + b_1(B(\hat{g}_e)\frac{\varphi(\hat{\theta}_f, x)}{\hat{g}})^2]S$$
$$+ B(\hat{g}_e)\frac{\varphi(\hat{\theta}_f, x)}{\hat{g}} - (1 - B(\hat{g}_e))\frac{\varphi(\hat{\theta}_f, x)}{g_m}$$

$$\cdot \tanh(\frac{S\varphi(\hat{\theta}_f, x)}{w_0}) \tag{42}$$

$$u = -k_z z + \dot{q} - Sg_u(x)\tanh(\frac{zSg_u(x)}{w_0}) \tag{43}$$

where $a_1, b_1 > 0$ are tunable constants and $\hat{g}_e = x_{n+1}\hat{\theta}_g^T \phi_g(x)$.

Instead of $B(\hat{g})$ in (29), the switching function $B(\hat{g}_e)$ is adopted in (42) for forming a prediction error term consistent with the upcoming CUA and hence enhancing the performance improvement.

By substituting (42)-(43) into (41), it yields the following closed-loop system

$$\begin{aligned}\dot{S} &= -\frac{g}{g_m}[k_s + a_1 g_u(x)^2 + b_1(B(\hat{g}_e)\frac{\varphi}{\hat{g}_e})^2]S \\ &\quad + \tilde{\theta}_f^T\phi_f + d(t) + g(x)(z + \nu(t)) + \frac{B(\hat{g}_e)}{\hat{g}}\tilde{g}\varphi \\ &\quad - (1 - B(\hat{g}_e))\varphi(1 + \frac{g(x)}{g_m}\tanh(\frac{S\varphi}{w_0})) \\ \dot{z} &= -k_z z - Sg_u(x)\tanh(\frac{zSg_u(x)}{w_0})\end{aligned} \tag{44}$$

It is reminded that the term $(B(\hat{g}_e)/\hat{g})\tilde{g}\varphi$ in (44) is actually equivalent to $(B(\hat{g}_e)/\hat{g}_e)\tilde{g}_e\varphi$, which will be used in the later stability analysis.

Remark 3: By picking up a sufficiently small τ_0 in (40), $\nu(t)$ can be made sufficiently small. Under such circumstances, the filter dynamics acts as the *fast dynamics* while the tracking error system (44) plus the upcoming parameter update algorithm are the *slow dynamics*. The $\nu(t)$ converges exponentially to the set $[-\varepsilon, \varepsilon]$ within the time interval $[0, T_1]$, where $\varepsilon, T_1 > 0$ can be made arbitrarily small via using sufficiently small τ_0. However, too small τ_0 nay ignite the peaking phenomenon in $\dot{q}(t)$ and hence initial spikes in $u(t)$ [21], [22]. On the other hand, larger τ_0 implies narrower filter's bandwidth. Larger $\nu(t)$ and hence spikes in $\dot{q}(t)$ may appear whenever faster variation of $\alpha(t)$ occurs. Those spikes then enter $u(t)$ for the inclusion of the cancelling term $\dot{q}$ in (43). Systematic guidelines for selecting the optimal τ_0 are unfortunately lacked so far. Consequently, some trial and error procedures should be taken in practice.

Remark 4: By a direct differentiation of $\nu(t)$.

$$\dot{\nu} = -\frac{1}{\tau_0}\nu - \dot{\alpha} \tag{45}$$

The solution $\nu(t)$ of (45) with $\nu(0) = 0$ is

$$\nu(t) = -\int_0^t e^{-\frac{1}{\tau_0}(t-\xi)}\dot{\alpha}(\xi)d\xi \tag{46}$$

Therefore, given positive numbers μ, T_q and a bounded C^1 function $\alpha(t)$ with $|\dot{\alpha}(t)| \leq \mu, \forall t \in [0, T_q]$, the bound for $\nu(t)$ can be estimated as

$$|\nu(t)| \leq \tau_0\mu(1 - e^{-T_q/\tau_0}). \tag{47}$$

As a consequence, given $\varepsilon > 0$, picking up a τ_0 within $(0, \delta]$, $\delta = \varepsilon/\mu$, one has (see Lemma 2 of [19])

$$|\nu(t)| \leq \varepsilon, \quad \forall t \in [0, T_q]. \tag{48}$$

Note that only the existence of δ can be ensured when the upper bound μ is unavailable. Such a property plays a key role in the subsequent stability analysis.

C. COMPOSITE UPDATE ALGORITHM

First, the x_n-subsystem in (1) is rewritten in a compact form of

$$\dot{x}_n = \theta^T\phi(x) + d(t), \tag{49}$$

where $\theta = col[\theta_f, \theta_g]$, $\phi = col[\phi_f, x_{n+1}\phi_g] \in R^{r+m}$.

Again, let

$$\hat{\theta}(t) = h(x_1, \cdots, x_n, x_{n+1}) + \vartheta(t), \tag{50}$$

where

$$h = \gamma\int_0^{x_n}\phi(x_1, \cdots, x_{n-1}, \xi, x_{n+1})d\xi, \tag{51}$$

and

$$\dot{\vartheta} = -\sum_{\substack{k=1 \\ k\neq n}}^{n+1}\frac{\partial h}{\partial x_k}\dot{x}_k + \gamma_0[S\bar{\psi}_s - \gamma_1(\hat{\theta}^T\phi)\phi] - \sigma\hat{\theta} \tag{52}$$

where $\bar{\psi}_s = col[\phi_f, (B(\hat{g}_e)\varphi/\hat{g})\phi_g]$.

By substituting (51)-(52) into (50), it yields

$$\dot{\hat{\theta}}(t) = \gamma_0[S\bar{\psi}_s + \gamma_1(\tilde{\theta}^T\phi + d(t))\phi] - \sigma\hat{\theta} \tag{53}$$

Remark 5: The state z in (39) is alternatively defined as $z = x_{n+1} - \alpha$ in a conventional backstepping design, with the corresponding error dynamics $\dot{z} = u - \dot{\alpha}$ [10], [20]. However, due to the dependence on x_{n+1} of $\hat{\theta}(t)$ in (50) and hence $\alpha(t)$ in (42), the term $(\partial\alpha/\partial x_{n+1})u(t)$ included in $\dot{\alpha}(t)$ will render the system uncontrollable when $1 - \partial\alpha/\partial x_{n+1} = 0$. In contrast, the introduced DSC scheme alleviates such drawbacks via filtering instead of differentiating $\alpha(t)$.

D. STABILITY ANALYSIS

Define two compact sets $\Omega_a = \{X|||X|| \leq r_a\}$ and $\Omega_b = \{X|||X|| \leq r_b\}$, with $X = col[x, x_{n+1}, q, \hat{\theta}] \in R^{n+r+m+2}$, $r_a > 0$, $x_d(t) \in \Omega_a$, $r_a < r_b$, and

$$\begin{aligned}\rho_3 &= \sqrt{\frac{(1 + c_3)\delta_3}{\gamma_1}} \\ \rho_4 &= \sqrt{\frac{(1 + c_4)(\epsilon^2 + 4c_a w_0 + a_1^{-1}\varepsilon^2 + 2b_1^{-1}\rho_3^2)}{k_{v,4}}}\end{aligned} \tag{54}$$

where $\delta_3 = (1 + \gamma_1)\epsilon^2 + (\sigma/\gamma_0)|\theta|^2 + 4c_a w_0 + (2/a_1)\varepsilon^2$, $c_a = 0.2785$, $a_1 > 0$ is a tunable constant, $0 < c_3, c_4 < 1$, and $k_{v,4} = \min[2k_s - 2b_1 - 1, 2k_z]$.

The main results are summarized in the following.

Theorem 2: Consider the extended system (41), the controller (43), the parametric estimator (50)-(52), and the filter dynamics in (40). For all $X(0) \in \Omega_a$, the following properties are ensured sustained Assumption 1-5 and $k_{v,4} > 0$, $\tau_0 \ll 1$.

P3: $x(t), x_{n+1}(t), q(t), \hat{\theta}(t), u(t) \in L_\infty, \forall t \geq 0$;

P4: There exist a finite positive number T_3 and a $T_4 \geq T_3$, such that

$$|\tilde{\theta}^T \phi(x)| \leq \rho_3, \quad \forall t \geq T_3, \tag{55}$$

and

$$|e_i(t)| \leq \frac{2^{i-1}}{\lambda_0^{n-i}} \rho_4, \quad \forall t \geq T_4, \tag{56}$$

where $1 \leq i \leq n$.

Proof:

Select the Lyapunov function

$$V_3 = \frac{1}{2}(S^2 + z^2 + \frac{1}{\gamma_0}\tilde{\theta}^T\tilde{\theta}) \tag{57}$$

Its time derivative along the closed-loop system (44) and (53) can be calculated as follows

$$\begin{aligned}\dot{V}_3 &= S\dot{S} + z\dot{z} - \frac{1}{\gamma_0}\tilde{\theta}^T\dot{\hat{\theta}} \\ &= S\{-\frac{g}{g_m}[k_s + a_1 g_u(x)^2 + b_1(B(\hat{g}_e)\frac{\varphi}{\hat{g}_e})^2]S \\ &\quad + \tilde{\theta}_f^T\phi_f + \frac{B(\hat{g}_e)}{\hat{g}}\tilde{g}\varphi + d(t) + g(x)(z + v(t)) \\ &\quad - (1 - B(\hat{g}_e))\varphi(1 + \frac{g(x)}{g_m}\tanh(\frac{S\varphi}{w_0}))\} \\ &\quad - k_z z^2 - zSg_u(x)\tanh(\frac{zSg_u(x)}{w_0}) \\ &\quad - \tilde{\theta}^T[S\bar{\psi}_s + \gamma_1(\tilde{\theta}^T\phi + d)\phi - \frac{\sigma}{\gamma_0}\hat{\theta}]\end{aligned} \tag{58}$$

First, it is noted that the term $S\tilde{\theta}^T\bar{\psi}_s$ cancels out $S(\tilde{\theta}_f^T\phi_f + B(\hat{g}_e)(\tilde{g}/\hat{g})\varphi)$. Next, by completing the squares, $Sd \leq 0.5(S^2 + \epsilon^2)$, $(\tilde{\theta}^T\phi)d \leq 0.5[(\tilde{\theta}^T\phi)^2 + \epsilon^2]$, $Sg(x)v(t) \leq (a_1 S^2 g_u(x)^2 + a_1^{-1}v^2(t))$, $\tilde{\theta}^T\hat{\theta} \leq \frac{1}{2}(-\tilde{\theta}^T\tilde{\theta} + ||\theta||^2)$, and recalling Lemma 1 of [23], $-S\varphi(1 + (g/g^m)\tanh(S\varphi/w_0)) \leq c_a w_0$, $Szg - zSg_u\tanh(zSg_u/w_0) \leq c_a w_0$. Then substituting them into (58), one has

$$\begin{aligned}\dot{V}_3 \leq -k_{v,3}V_3 - \frac{\gamma_1}{2}(\tilde{\theta}^T\phi)^2 + \frac{1}{2}\{\frac{\sigma}{\gamma_0}||\theta||^2 + (1+\gamma_1)\epsilon^2 \\ + 4c_a w_0 + \frac{2}{a_1}v^2(t)\},\end{aligned} \tag{59}$$

where $k_{v,3} = \min[2k_s - 1, 2k_z, \sigma]$.

Now, since the righthand sides of (44) and (53) are bounded for bounded X, there exists a $T_b > 0$, such that $X(t) \in \Omega_b, \forall X(0) \in \Omega_a, t \in [0, T_b]$. Meanwhile, $\alpha(t)$ in (42) is apparently bounded $\forall t \in [0, T_b]$. Based on Remark 4, given $\varepsilon > 0$, there exists a $\delta > 0$, such that $|v(t)| \leq \varepsilon, \forall t \in [0, T_b], \tau_0 \in (0, \delta]$. As a result,

$$\dot{V}_3 \leq -k_{v,3}V_3 - \frac{\gamma_1}{2}(\tilde{\theta}^T\phi)^2 + \frac{\delta_3}{2}, \quad \forall t \in [0, T_b] \tag{60}$$

It implies that

$$\begin{aligned}V_3(t) &\leq V_3(0)e^{-k_{v,3}t} + \frac{\delta_3}{2k_{v,3}}(1 - e^{-k_{v,3}t}) \\ &\leq \max[V_3(0), \frac{\delta_3}{2k_{v,3}}], \quad \forall t \in [0, T_b]\end{aligned} \tag{61}$$

Denote $c_v = \min V_3(X), \forall X \in \partial\Omega_b$, where $\partial\Omega_b$ is the set of boundary points of Ω_b. By selecting a r_b such that $c_v > \max_{X(0)\in\Omega_a}[V_3(0), \delta_3/(2k_{v,3})]$, then T_b can be extended to ∞. The boundedness of $X(t)$ and hence $u(t)$ follows immediately and therefore P3 is thus proven.

Next, since $\dot{V}_3$ in (60) is in the same form of (18), by similar reasoning, it can be easily concluded that there exists a $T_3 > 0$, such that $|\tilde{\theta}^T\phi|$ ultimately converges to ρ_3 for all $t \geq T_3$. (55) is thus proven.

To prove (56), consider the Lyapunov function $V_4(S, z) = 0.5(S^2 + z^2)$. Its time derivative along (44) can be calculated as

$$\begin{aligned}\dot{V}_4 &= S\dot{S} + z\dot{z} \\ &\leq -[k_s - \frac{1}{2} + b_1(B(\hat{g}_e)\frac{\varphi}{\hat{g}_e})^2]S^2 \\ &\quad + S(\tilde{\theta}_f^T\phi_f + B(\hat{g}_e)\frac{\tilde{g}}{\hat{g}}\varphi) - k_z z^2 \\ &\quad + \frac{1}{2}((1+\gamma_1)\epsilon^2 + 4c_a w_0 + \frac{2}{a_1}\varepsilon^2)\end{aligned} \tag{62}$$

Again, by completing the squares, $S(\tilde{\theta}_f^T\phi_f) \leq b_1 S^2 + b_1^{-1}(\tilde{\theta}_f^T\phi_f)^2$, $SB(\hat{g}_e)(\tilde{g}/\hat{g})\varphi = SB(\hat{g}_e)(\tilde{g}_e/\hat{g}_e)\varphi \leq b_1(B(\hat{g}_e)\varphi/\hat{g}_e)^2 S^2 + b_1^{-1}\tilde{g}_e^2$ and then substituting them into (62), it yields

$$\begin{aligned}\dot{V}_4 &\leq -k_{v,4}V_4 + \frac{1}{b_1}((\tilde{\theta}_f^T\phi_f)^2 + \tilde{g}_e^2) \\ &\quad + \frac{1}{2}(\epsilon^2 + 4c_a w_0 + \frac{2}{a_1}\varepsilon^2) \\ &\leq -k_{v,4}V_4 + \frac{\delta_4}{2}, \quad \forall t \geq T_3\end{aligned} \tag{63}$$

where $\delta_4 = \epsilon^2 + 4c_a w_0 + (2/a_1)\varepsilon^2 + (2/b_1)\rho_3^2$.

Therefore, there exists a $T_4 \geq T_3$, such that

$$|S(t)| \leq \sqrt{\frac{(1+c_4)\delta_4}{k_{v,4}}}, \quad \forall t \geq T_4 \tag{64}$$

The results in (56) follows immediately [1].

V. SIMULATION

In this section, two case studies are presented for demonstrating the validity of the proposed designs.

Case 1 (Known g): The proposed I&I-based CAC design in (4) and (10)-(12) is compared with the LBUA-based design in (4) and (6) herein. Consider the following linearisable system

$$\begin{aligned}\dot{x}_1 &= x_2, \\ \dot{x}_2 &= g(x)u + \theta_f^T\phi_f(x) + d(t),\end{aligned} \tag{65}$$

where $x = [x_1, x_2]^T$, $\theta_f = [5, 4, 3]^T$, $\phi_f = [x_1 x_2^2\sin(3x_2^3), x_1^3\exp(2x_2), x_1 x_2]^T$, $g(x) = 3(1 + x_1^2 e^{-x_2}) + \cos(x_1 + 1) + 0.5\sin(2x_1 + x_2)$, and $d(t) = 0.2\sin(10t)$.

Since $\phi_f(x)$ is integrable with respect to x_2, the integration in (11) can be carried out to yield

$$h_f(x) = \gamma[-\frac{x_1}{3}\cos(3x_2^3), \frac{x_1^3}{2}e^{2x_2}, \frac{x_1}{2}x_2^2]^T \tag{66}$$

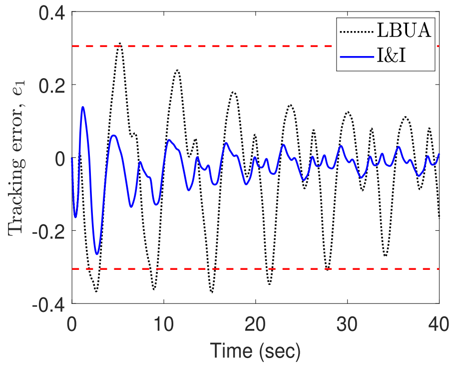

FIGURE 1. Comparison of tracking error $e_1(t)$ in Case 1.

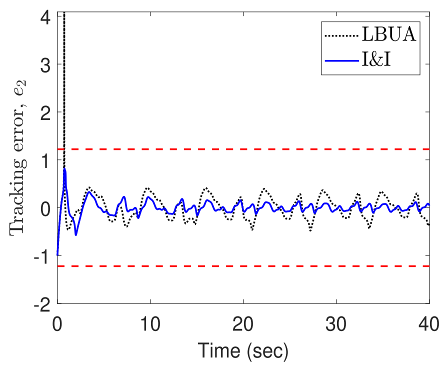

FIGURE 2. Comparison of tracking error $e_2(t)$ in Case 1.

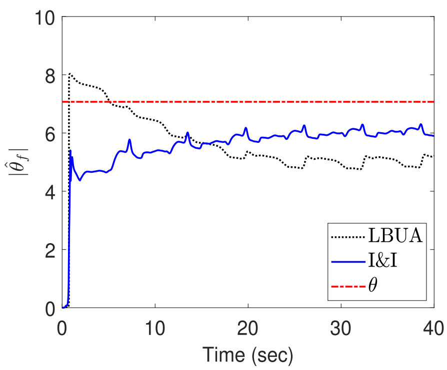

FIGURE 3. Comparison of parametric error $|\tilde{\theta}_f(t)|$ in Case 1.

The reference trajectory is $y_d = \sin(t)$. The adopted numerical values are $\lambda_0 = 2.0, k_s = 2.0. \gamma_0 = \gamma_1 = 1.0, \sigma = 0.01$, and $x(0) = \vartheta_f(0) = 0$. By choosing $c_1 = c_2 = 0.1$, the upper bounds for $|\tilde{\theta}_f^T \phi_f(x)|$ in (15) and $|e_i(t)|$ in (16) are $\rho_1 = 0.7987$ and $\rho_2 = 0.6107 * 2^{2i-3}$, $i = 1, 2$, respectively.

The simulation results are shown in Figures 1-5. The tracking errors $e_1(t)$ and $e_2(t)$ of the proposed CAC design are well bounded respectively by 0.3053 and 1.2214 (the red-dashed lines) in Figure 1 and Figure 2, respectively. In contrast, the standard LUBA not only takes longer time to converge into the respective zones, but also with larger tracking errors along the way. Next, the estimated parameters $|\hat{\theta}_f|$ in Figure 3 and the prediction errors $\tilde{\theta}_f^T \phi_f(x)$

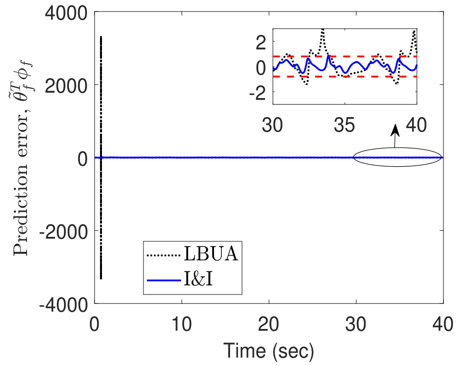

FIGURE 4. Comparison of prediction error $\tilde{\theta}_f^T \phi_f(t)$ in Case 1.

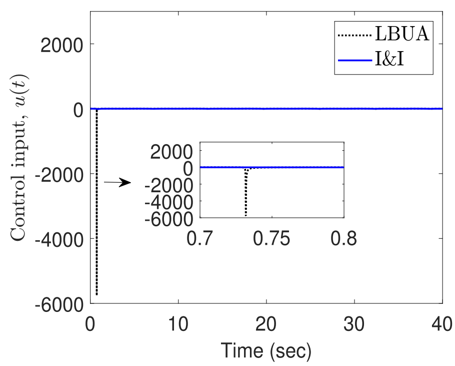

FIGURE 5. Comparison of control input $u(t)$ in Case 1.

in Figure 4 demonstrate the same discrepancy between the two schemes. Noticeably, although both $|\hat{\theta}_f(t)|$ do not converge to $|\theta_f|$, nevertheless, $\tilde{\theta}_f^T \phi_f(x)$ of the proposed method are ultimately bounded by ± 0.7987, the red-dashed lines in Figure 4, while the latter fails to fulfill such a criterion. Finally, the poor transient peaks in $u(t)$ of the LBUA in Figure 5 demonstrated again the superiority of the proposed CAC design.

Case 2 (Unknown g): Next, simulation on a practical brushless DC motor with unknown input gain functions will be conducted herein. Neglecting the dynamics of the electrical subsystem, the system dynamics can be modeled by [24]

$$\begin{aligned} \dot{x}_1 &= x_2 \\ \dot{x}_2 &= \frac{1}{M}[(K_{F0} + K_{Fx}(x_1))\frac{u}{R} - Bx_2 \\ &\quad + f_{fric}(x_2) + f_{cog}(x_1) + f_{dis}(t)] \end{aligned} \tag{67}$$

where x_1 is the displacement, x_2 is the velocity, u is the control input voltage, M is the mass of the inertia, R is the resistance, B is the combined coefficient of the damping and viscous friction on the load, $K_{F0} > 0$ is an unknown constant, $f_{fric}(x_2)$ is the friction force modeled by $f_{fric}(x_2) = -f_c \tanh(a_c x_2)$, with $f_c, a_c > 0$, $f_{dis}(t)$ is the bounded disturbance, while $K_{Fx}(x_1)$ and $f_{cog}(x_1)$ are periodic functions in a form of

$$\begin{aligned} f_{cog}(x_1) &= A_c^T S_c(x_1) \\ K_{Fx}(x_1) &= A_K^T S_K(x_1) \end{aligned}$$

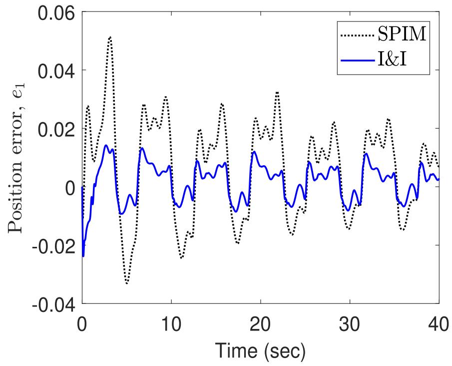

FIGURE 6. Comparison of position error $e_1(t)$ in Case 2.

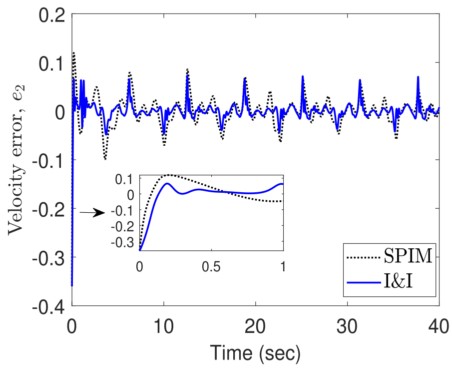

FIGURE 7. Comparison of velocity error $e_2(t)$ in Case 2.

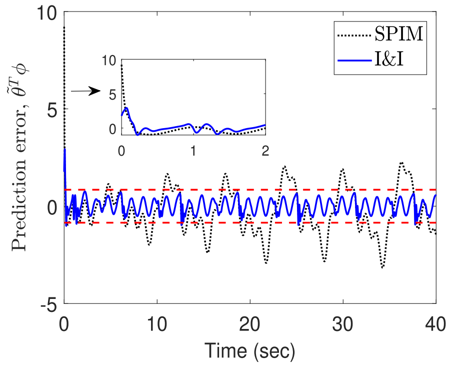

FIGURE 8. Comparison of prediction error $\tilde{\theta}^T\phi(t)$ in Case 2.

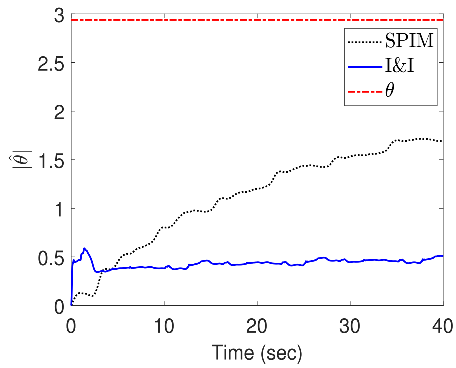

FIGURE 9. Comparison of parametric error $|\tilde{\theta}(t)|$ in Case 2.

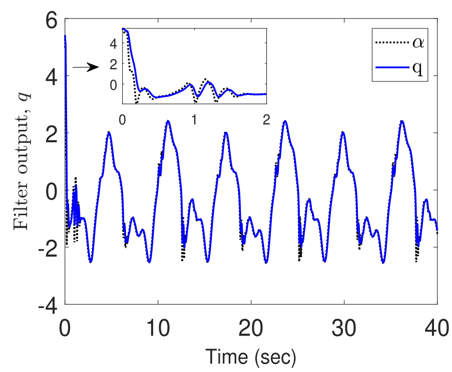

FIGURE 10. Filter input $\alpha(t)$ and output $q(t)$ in Case 2.

where $A_c = [A_{c,1}, \cdots, A_{c,\rho_a}]^T$, $A_K = [A_{K,1}, \cdots, A_{K,\rho_b}]^T$ are the unknown weights, $S_c = [\sin(\frac{2\pi x_1}{T_x}), \cos(\frac{2\pi x_1}{T_x}), \cdots, \sin(\frac{2\pi\rho_a x_1}{T_x}), \cos(\frac{2\pi\rho_a x_1}{T_x})]^T$ and $S_K = [\sin(\frac{2\pi x_1}{T_x}), \cos(\frac{2\pi x_1}{T_x}), \cdots, \sin(\frac{2\pi\rho_b x_1}{T_x}), \cos(\frac{2\pi\rho_b x_1}{T_x})]^T$ are the known basis vector functions, with $T_x > 0$ being the known period.

The proposed I&I-based CAC design in (43) and (50)-(52) is now compared with the standard SPIM-based CAC in (29) and (34)-(35). Rewrite $g(x)$ in a linearly parameterized form of $g(x) = \theta_g^T\phi_g$, $\theta_g = col[K_{F0}, A_{K,1}, \cdots, A_{K,\rho_b}]/(MR)$ with $\phi_g = col[1, \sin(\frac{2\pi x_1}{T_x}), \cdots, \sin(\frac{2\pi\rho_b x_1}{T_x}), \cos(\frac{2\pi\rho_b x_1}{T_x})]$, $f(x) = \theta_f^T\phi_f$, $\theta_f = col[-B, -f_c, A_{c,1}, \cdots, A_{c,\rho_a}]/M$ and $\phi_f = col[x_2, \tanh(a_c x_2), \sin(\frac{2\pi x_1}{T_x}), \cdots, \cos(\frac{2\pi\rho_a x_1}{T_x})]$. The lumped parameter vector and the basis vector function are $\theta = col[\theta_f, \theta_g]$ and $\phi = col[\phi_f, x_3\phi_g]$, respectively. The integration in (47) can be explicitly calculated to yield

$$h(x) = \gamma[0.5x_2^2, \frac{1}{a_c}\ln\cosh(a_c x_2), \sin(\frac{2\pi x_1}{T_x})x_2, \cdots, \sin(\frac{2\pi\rho_a x_1}{T_x})x_2, x_2x_3, \sin(\frac{2\pi x_1}{T_x})x_2x_3, \cdots, \sin(\frac{2\pi\rho_b x_1}{T_x})x_2x_3]^T \quad (68)$$

The reference trajectory is changed to $y_d = 0.3\sin(t)(1 + 0.2\cos(0.5t))$, while the extra numerical values are: $M = 10kg$. $B = 0.5N/m/s$, $K_{F0} = 55.5N/A$, $R = 3.9\Omega$, and $T_x = 1.0m$. For simplicity, we choose $f_{cog} = 25\sin(\frac{2\pi x_1}{T_x} + \frac{\pi}{4})N$, $K_{Fx} = 1.11\sin(\frac{2\pi x_1}{T_x} + \frac{\pi}{4})$, $f_c = 6, a_c = 5$, $f_{dis}(t) = 0.5\sin(5t)$, $\lambda_0 = k_s = k_z = 5.0$, and $\tau_0 = 0.05$. By choosing $c_3 = c_4 = 0.5$, the upper bounds for $|\tilde{\theta}^T\phi(x)|$ in (55) and $|e_i(t)|$ in (56) are $\rho_3 = 0.8466$ and $\rho_4 = 1.3567 * 2^{2i-3}$, $i = 1, 2$, respectively.

The simulation results are shown in Figures 6-12. The proposed design exhibits better tracking performance in e_1 of Figure 6 and e_2 of Figure 7 than the SPIM-based scheme. Next, in contrast to the latter, the prediction errors $\tilde{\theta}^T\phi$ of the proposed design converge quickly to fulfill $|\tilde{\theta}^T\phi| \leq 0.8466$ marked by the two red-dashed lines in Figure 8. On the other hand, the estimated parameters in Figure 9 did not reflect such a trend. It verifies that the tracking performance

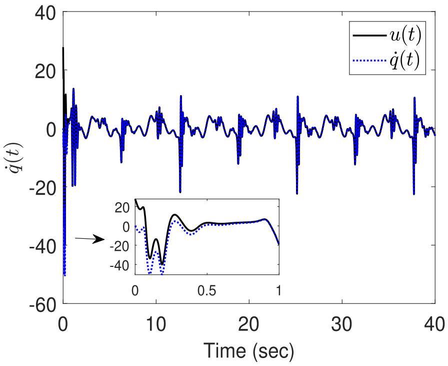

FIGURE 11. Trajectories of $u(t)$ and $\dot{q}(t)$ in Case 2.

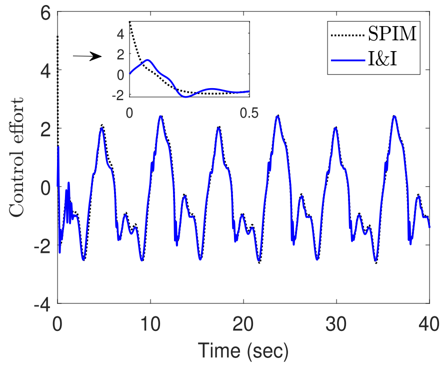

FIGURE 12. Comparison of $u(t)$ of SPIM-based and $x_3(t)$ of I&I based schemes in Case 2.

improvement of the proposed design does not rely on the parameter convergence.

By using $\tau_0 = 0.05 \ll 1$, the filter output $q(t)$ and the virtual control $\alpha(t)$ in Figure 10 almost coincide, meaning that $\varepsilon \ll 1$. As mentioned in Remark 3, large $\dot{q} = (\alpha - q)/\tau_0$ and consequently large $u(t)$ occurs when rapid variation in $\alpha(t)$ appears in Figure 11. In view of the extended system (37), it should be cautious that the actual input force to the x_2 dynamics is the extended state x_3, i.e. $\int_0^t u(\tau)d\tau$, instead of $u(t)$ itself. A comparison of control efforts between $u(t)$ of the SPIM-based scheme and $x_3(t)$ of the proposed design is depicted in Figure 12. They are about the same magnitudes, implying that the proposed design does not consume excessive control efforts in this application. On the other hand, the oscillatory portion of the input force $x_3(t)$ around $t = 1$ *sec* in Figure 12 will produce corresponding oscillatory acceleration signal $\dot{x}_2$ for the system (67) and hence similar velocity response in Figure 7. It in turn leads to oscillatory behaviors in $\tilde{\theta}^T \phi(x)$ for the dependence on x_2 of $\phi(x)$.

VI. CONCLUSION

Adaptive control designs for linearisable systems with known or unknown input-gain functions are not new at all. However, they generally suffered from the previously mentioned two drawbacks D1 and D2, which remains open so far. The proposed designs conquer such drawbacks and hence improve the identification and the tracking performance simultaneously. For the cases with unknown input-gain functions, the adding an integrator technique, the DSC scheme, and the smooth switching algorithm are incorporated together for solving the algebraic-loop and control-singularity problems simultaneously. Simulation works have demonstrated its effectiveness and superiority over the existing designs. Most of all, the achievement does not rely on the parameter convergence and hence the corresponding excitation criteria on the regressor vector. It is appealing to practical applications in this respect.

Despite these achievements, there are some topics worth of further investigations, such as prevention of high-gain effects in the filter dynamics, systematic guidelines for the gain selections, and output-feedback control, etc. Moreover, extension of such an approach to more general nonlinear systems is also quite challenging. To start with, some existing works are noticeable, such as [10], [19], [21], [22], [25]. We are encouraged to tackle the aforementioned tasks in the near future.

ACKNOWLEDGMENT

The author is really grateful to the Editor, the Associate Editor, and the reviewers for their insightful comments.

REFERENCES

[1] J.-J. E. Slotine and W. Li, *Applied Nonlinear Control*. Englewood Cliffs, NJ, USA:Prentice-Hall, 1991.
[2] P. A. Ioannou and J. Sun, *Robust Adaptive Control*. Upper Saddle River, NJ, USA: Prentice-Hall, 1996.
[3] M. Kemal Ciliz, "Combined direct and indirect adaptive control for a class of nonlinear systems," *IET Control Theory Appl.*, vol. 3, no. 1, pp. 151–159, Jan. 2009.
[4] K. Y. Volyanskyy, W. M. Haddad, and A. J. Calise, "A new neuroadaptive control architecture for nonlinear uncertain dynamical systems: Beyond σ- and e-modifications," *IEEE Trans. Neural Netw. Learn. Syst.*, vol. 20, no. 11, pp. 1707–1723, Nov. 2009.
[5] P. M. Patre, W. MacKunis, M. Johnson, and W. E. Dixon, "Composite adaptive control for Euler–Lagrange systems with additive disturbances," *Automatica*, vol. 46, no. 1, pp. 140–147, Jan. 2010.
[6] J. Chen, Z. Li, G. Zhang, and M. Gan, "Adaptive robust dynamic surface control with composite adaptation laws," *Int. J. Adapt. Control Signal Process.*, vol. 24, no. 12, pp. 1036–1050, Dec. 2010.
[7] B. Xu, Z. Shi, C. Yang, and F. Sun, "Composite neural dynamic surface control of a class of uncertain nonlinear systems in strict-feedback form," *IEEE Trans. Cybern.*, vol. 44, no. 12, pp. 2626–2634, Dec. 2014.
[8] L.-X. Wang, "Design and analysis of fuzzy identifiers of nonlinear dynamic systems," *IEEE Trans. Autom. Control*, vol. 40, no. 1, pp. 11–23, Jan. 1995.
[9] Y. Pan and H. Yu, "Composite learning from adaptive dynamic surface control," *IEEE Trans. Autom. Control*, vol. 61, no. 9, pp. 2603–2609, Sep. 2016.
[10] A. Astolfi, D. Karagiannis, and R. Ortega, *Nonlinear and Adaptive Control With Applications*. London, U.K.: Springer-Verlag, 2008.
[11] A. Astolfi and R. Ortega, "Immersion and invariance: A new tool for stabilization and adaptive control of nonlinear systems," *IEEE Trans. Autom. Control*, vol. 48, no. 4, pp. 590–606, Apr. 2003.
[12] J.-T. Huang, "An adaptive compensator for a class of linearly parameterized systems," *IEEE Trans. Autom. Control*, vol. 47, no. 3, pp. 483–486, Mar. 2002.
[13] S. Aranovskiy, A. Bobtsov, R. Ortega, and A. Pyrkin, "Performance enhancement of parameter estimators via dynamic regressor extension and mixing," *IEEE Trans. Autom. Control*, vol. 62, no. 7, pp. 3546–3550, Jul. 2017.
[14] D. Efimov, N. Barabanov, and R. Ortega, "Robust stability under relaxed persistent excitation conditions," in *Proc. 57th IEEE Conf. Decis. Control*, Miami Beach, FL, USA, Dec. 2018, pp. 7243–7248.

[15] J. Wang, D. Efimov, and A. A. Bobtsov, ''On robust parameter estimation in finite-time without persistence of excitation,'' *IEEE Trans. Autom. Control*, vol. 65, no. 4, pp. 1731–1738, Apr. 2020.
[16] J. M. Coron and L. Praly, ''Adding an integrtor for the stabilization problem,'' *Syst. Control Lett.*, vol. 17, no. 2, pp. 89–104, 1991.
[17] T. E. Gibson, A. M. Annaswamy, and E. Lavretsky, ''On adaptive control with closed-loop reference models: Transients, oscillations, and peaking,'' *IEEE Access*, vol. 1, pp. 703–717, 2013.
[18] J.-T. Huang, ''Hybrid-based adaptive NN backstepping control of strict-feedback systems,'' *Automatica*, vol. 45, no. 6, pp. 1497–1503, Jun. 2009.
[19] W. J. Dong, J. A. Farrell, M. Polycarpou, V. Djapic, and M. Sharma, ''Command fitered adaptive backstepping,'' *IEEE Trans. Control Syst. Technol.*, vol. 20, no. 3, pp. 566–580, May 2012.
[20] M. Krstic, I. Kanellakopoulos, and P. V. Kokotovic, *Nonlinear and Adaptive Control Design*. New York, NY, USA: Wiley, 1995.
[21] H. K. Khalil, *Nonlinear Control*. Upper Saddle River, NJ, USA: Prentice-Hall, 2015.
[22] A. Levant, ''Higher-order sliding modes, differentiation and output-feedback control,'' *Int. J. Control*, vol. 76, nos. 9–10, pp. 924–941, Jan. 2003.
[23] M. M. Polycarpou, ''Stable adaptive neural control scheme for nonlinear systems,'' *IEEE Trans. Autom. Control*, vol. 41, no. 3, pp. 447–451, Mar. 1996.
[24] B. Yao and L. Xu, ''Adaptive robust control of linear motors for precision manufacturing,'' *IFAC Proc. Volumes*, vol. 32, no. 2, pp. 25–30, Jul. 1999.
[25] W. Deng, J. Yao, Y. Wang, X. Yang, and J. Chen, ''Output feedback backstepping control of hydraulic actuators with valve dynamics compensation,'' *Mech. Syst. Signal Process.*, vol. 158, Sep. 2021, Art. no. 107769.

JENG-TZE HUANG (Member, IEEE) was born in Taichung, Taiwan. He received the B.Sc. degree in mechanical engineering from National Central University, Taiwan, in 1984, the M.S. degree in electrical engineering from National Taiwan University, Taiwan, in 1986, and the Ph.D. degree in electrical and control engineering from National Chiao Tung University, Taiwan, in 1998. He was with the Department of Electronic Engineering, Vanung University of Technology, Taiwan, from 1990 to 2007. He was with the Institute of Digital Mechatronic Technology, Chinese Culture University, Taipei, as an Institute Director, from 2011 to 2016, where he is currently a Professor. His current research interests include nonlinear control, adaptive control, intelligent control, and robotics.

YU-WEI JIANG was born in Keelung, Taiwan, in 1999. He received the B.S. degree in mechanical engineering from Chinese Culture University, Taipei, Taiwan, in 2020, where he is currently pursuing the M.S. degree in mechanical engineering. His research interests include mechatronics, automatic control, and unmanned aerial vehicles.